https://doi.org/10.5194/egusphere-2026-2453
Preprint. Discussion started: 12 June 2026
© Author(s) 2026. CC BY 4.0 License.

How atmospheric and surface conditions shape recurrent heatwaves in Europe: From local to continental scales

Ines Dillerup[1], Gabriele Messori[2,3,4], Alexander Lemburg[1], Sebastian Buschow[5,6], and Joaquim G. Pinto[1]

[1]Institute for Meteorology and Climate Research - Troposphere Research (IMKTRO), Karlsruhe Institute of Technology (KIT), Karlsruhe, Germany
[2]Department of Earth Sciences, Uppsala University, Uppsala, Sweden
[3]Swedish Centre for Impacts of Climate Extremes (climes), Uppsala University, Uppsala, Sweden
[4]Department of Meteorology, Stockholm University, Stockholm, Sweden
[5]Institute of Geosciences, University of Bonn, Bonn, Germany
[6]Jülich Supercomputing Centre, Forschungszentrum Jülich, Jülich, Germany

Correspondence: Ines Dillerup (ines.dillerup@kit.edu)

Abstract. Heatwaves are among the most impactful climate extremes in Europe. Their recurrence, defined as sequences of heatwaves separated by short breaks, is projected to increase disproportionately under climate change, yet remains poorly understood. This is in part because recurrence emerges from interacting processes operating across spatial scales, from local land–atmosphere feedbacks to large-scale atmospheric circulation, and studies often focus on only one scale at a time. We develop a unified framework to investigate heatwave recurrence across local, object, and continental scales over Europe using the European Centre for Medium-Range Weather Forecasts ERA5 reanalysis for 1950–2024.

Our results reveal complementary insights at each spatial scale. Local recurrence, that is heatwaves at one location separated by less than seven days, exhibit weaker daily temperature and soil moisture anomalies than isolated events. However, recurrent heatwave objects, defined as spatially contiguous heatwave objects corresponding to strong local recurrence, show higher soil moisture depletion and higher temperatures compared to single events. They further persist longer, cover larger areas, and are more frequently associated with European blocking in July and August. Continental recurrence reflects summers in which multiple heatwave objects overlap spatially, affecting large areas or striking the same regions repeatedly. It emerges as a distinct dimension of summer heat extremes rather than simply reflecting anomalously warm conditions. Summers with high continental recurrence feature more heatwaves, larger affected areas, higher temperature anomalies, and earlier, more persistent soil moisture depletion compared to summers with isolated events. Further, despite some overlap between high continental and high local recurrence, both represent distinct and complementary perspectives on heatwave recurrence.

These findings demonstrate that recurrence is a cross-scale phenomenon and highlight the importance of integrating complementary spatial perspectives to better understand compound heat extremes and the coupled atmospheric–land surface processes that govern them.

https://doi.org/10.5194/egusphere-2026-2453
Preprint. Discussion started: 12 June 2026
© Author(s) 2026. CC BY 4.0 License.

1 Introduction

Weather and climate extremes such as heatwaves pose an increasingly severe burden on human health, ecosystems, and economies worldwide (Calvin et al., 2023). Even modest increases in mean temperature can lead to disproportionately large increases in the frequency, intensity, and spatial extent of extreme heat events (Perkins, 2015; León-FonFay et al., 2026). In particular, Europe has emerged as a hotspot for heatwaves under ongoing climate change (Perkins, 2015; Barriopedro et al., 2023). As extreme events can exceed the coping capacity of natural and human systems, understanding the physical processes that drive their occurrence remains a key scientific challenge (Calvin et al., 2023). Accurate prediction and attribution of heatwaves are therefore essential, yet they depend on a detailed understanding of the complex interactions among atmospheric circulation, land–atmosphere coupling, and background climate conditions.

Heatwaves arise from the interplay between large-scale atmospheric circulation anomalies and land–surface processes (Barriopedro et al., 2023). In Europe, heatwaves are frequently associated with persistent anticyclonic circulation patterns, including atmospheric blocking, which inhibit the zonal propagation of weather systems and promote subsidence, clear-sky conditions, and warm air advection (Santos et al., 2015; Bieli et al., 2015; Kautz et al., 2022; Lemburg et al., 2026; Dillerup et al., 2026). Land–atmosphere interactions, particularly soil moisture–temperature feedbacks, can further amplify heat extremes by limiting evaporative cooling and enhancing sensible heat fluxes, with the strength of this coupling depending on antecedent soil moisture conditions and varying across regions and events (Seneviratne et al., 2010; Liu et al., 2020; Benson and Dirmeyer, 2021; Maraun et al., 2025). When such processes persist or recur in close succession, heatwaves may exhibit a compound nature, as earlier events can precondition the land surface and amplify subsequent extremes.

While the characteristics and drivers of individual heatwaves have been widely studied, comparatively little attention has been paid to recurrent heatwaves, that is, repeated heatwave occurrences separated by short breaks (Hughes et al., 2018; Baldwin et al., 2019; Zhang et al., 2025). Importantly, the relative roles of atmospheric circulation and land–surface feedbacks in governing recurrent heatwave behavior remain incompletely understood (Zscheischler et al., 2020; Barriopedro et al., 2023). This research gap is notable, as heatwave sequences are projected to increase disproportionately in a warming climate, even beyond the increase in single events (Baldwin et al., 2019; Zhang et al., 2025). In addition, global warming may extend the heatwave season in Central Europe into October (Hundhausen et al., 2023), further enhancing the potential for prolonged heatwave sequences. From an impact perspective, such sequences are particularly critical: an initial heatwave can precondition the land surface, heighten vulnerability, and reduce recovery capacity, thereby amplifying the impacts of subsequent events on health, ecosystems, and infrastructure (Hughes et al., 2018). It has further been shown that sequences of heatwaves interact with the urban heat island (Zhang et al., 2025).

Despite their growing relevance, recurrent heatwaves over Europe remain insufficiently understood. Previous studies have largely focused either on individual events or on grid-cell-based recurrence (Baldwin et al., 2019; Zhang et al., 2025), making it difficult to disentangle local cumulative impacts from the dynamics of spatially coherent heatwave objects. A comprehensive understanding of recurrent heatwaves and their links to atmospheric circulation, land–atmosphere interactions, and impacts

https://doi.org/10.5194/egusphere-2026-2453
Preprint. Discussion started: 12 June 2026
© Author(s) 2026. CC BY 4.0 License.

instead requires an explicit consideration of multiple spatial scales. However, to our knowledge, no study has systematically examined recurrent heatwaves over Europe across multiple spatial scales.

To address this gap, we introduce a unified framework that integrates grid-cell-based recurrence, object-based heatwaves, and continental-scale recurrence. At the local scale, recurrence manifests as repeated temperature exceedances at a fixed location separated by short breaks. This perspective captures land-atmosphere recovery processes, such as soil moisture replenishment, and directly reflects cumulative exposure relevant for human health, ecosystems, and agriculture. However, observing recurrence at a single location does not reveal why certain regions experience repeated extremes. Heatwaves are not purely local phenomena; they are shaped by large-scale atmospheric circulation patterns that organize temperature anomalies over broad areas (Kautz et al., 2022; Barriopedro et al., 2023). To relate local recurrence to these dynamical drivers, an intermediate scale is needed. We therefore introduce an object-based perspective, in which adjacent or nearby exceedances are grouped into coherent heatwave objects. This scale makes it possible to distinguish between heatwave objects that generate repeated local extremes and those that do not. In this way, local cumulative exposure can be linked to the properties and dynamics of spatially coherent events. Beyond individual objects, recurrence can also emerge from the succession of multiple heatwave systems within a single summer. At the continental scale, this reflects the seasonal organization of extreme heat across Europe. High continental recurrence can indicate either that large areas of the continent are affected by multiple heatwaves or that smaller regions experience repeated heatwaves.

This approach allows us to capture the multifaceted nature of recurrent heatwave activity and its links to atmospheric circulation and land–atmosphere interactions, as each spatial scale highlights complementary aspects of recurrence. By explicitly distinguishing recurrence across spatial scales, the study aims to improve understanding of the frequency, timing, and spatial organization of recurrent heatwaves, providing a more nuanced picture of extreme heat in a warming climate.

In particular, this study addresses the following research questions:

- Local scale: How do locally recurrent heatwaves differ from isolated heatwaves in terms of temperature and soil-moisture anomalies?
- Object scale: Which physical characteristics and atmospheric circulation patterns distinguish heatwave objects with strong versus weak local recurrence?
- Continental scale: How does the recurrence of heatwave objects within a summer shape their characteristics across Europe, and how does continental-scale recurrence relate to local heatwave recurrence?

Section 2 describes the data, indices, and methods for computing recurrent heatwaves accross spatial scales. Section 3.1 analyzes local-scale recurrence and regional variability, Section 3.2 assesses object-scale characteristics and atmospheric circulation patterns, and Section 3.3 examines continental-scale differences between summers. Section 4 summarizes the findings and their implications.

https://doi.org/10.5194/egusphere-2026-2453
Preprint. Discussion started: 12 June 2026
© Author(s) 2026. CC BY 4.0 License.

2 Data and Methods

2.1 Data

We used the ERA5 reanalysis dataset provided by the European Center for Medium-Range Weather Forecasts (ECMWF) over the period 1950-2024 on a 31km grid. The chosen domain spans 11°W-30°E, 40-60°N to focus on Central Europe. The considered variables are: daily maximum temperature (tasmax) and soil moisture in the upper soil level (0-7cm) (swvl1). Daily means were computed for swvl1, and anomalies were defined for both tasmax and swlv1 relative to a smoothed daily climatology using a 21-year running window mean.

2.2 Weather regimes

Weather regimes are used to characterize low-frequency variability of the large-scale atmospheric circulation (Hannachi et al., 2017) associated with recurrent heatwaves. We employ the year-round weather regime classification of Grams (2026), derived from ERA5 geopotential height anomalies at 500 hPa over the Atlantic–European sector (80°W–40°E, 30°N–90°N). The classification is based on EOF analysis and k-means clustering of normalized, low-pass-filtered Z500 anomalies and identifies seven canonical regimes: three cyclonic regimes (Atlantic Trough, Zonal, Scandinavian Trough) and four blocked regimes (Atlantic Ridge, European Blocking, Scandinavian Blocking, Greenland Blocking). The Zonal and Greenland Blocking regimes are related to the positive and negative phases of the North Atlantic Oscillation, respectively. The regime patterns are displayed in Supplementary Figure S1.

For each time step, the similarity between instantaneous Z500 anomalies and the regime patterns is quantified using the weather regime index I_{wr} (Michel and Rivière, 2011). Following Grams (2026), active weather regime occurrences are identified from periods of sustained high similarity, and each day is assigned to the dominant weather regime or to a no-regime category.

2.3 Heatwave definition

A variety of methods exist to detect heatwaves (Robinson, 2001; Perkins and Alexander, 2013; Russo et al., 2015; Becker et al., 2022; Messori et al., 2024), which all require the exceedance of a temperature threshold. To remove the long-term warming trend, we first detrend daily maximum temperatures in each grid cell using a second-order polynomial. Then we follow the procedure for the HWMid index (Russo et al., 2015) by computing the 90th percentile of the detrended daily maximum anomalies for each grid cell using a 31-day running window over the 1991–2020 reference period. A heatwave is defined as a sequence of at least three days exceeding this threshold. We further allow for a single non-exceedance day within the sequence.

While this heatwave detection provides a robust grid-point–level definition, our aim to connect heatwaves to the large-scale atmospheric circulation requires a complementary spatial approach, in which geographically contiguous heatwave regions are constructed from adjacent heatwave grid points following Messori et al. (2024). At each timestep, regions consisting of four or fewer connected grid cells are discarded. This is consistent with previous studies that removed isolated grid cells at coarser

https://doi.org/10.5194/egusphere-2026-2453
Preprint. Discussion started: 12 June 2026
© Author(s) 2026. CC BY 4.0 License.

spatial resolution (1°), and serves to suppress grid-scale noise. For each group of neighboring heat wave grid cells, a centroid is computed. If the distance between the centroids is smaller than 1000 km, the regions are merged into one, as it is not expected that different physical drivers lead to geographically contiguous heatwaves. Finally, a minimum area criterion of $2*10^5 km^2$ is applied. The remaining heatwaves at each grid cell are referred to as (local) heatwaves throughout this study.

2.4 Heatwave object definition

To define heatwave objects, we track geographically contiguous heatwave regions across multiple timesteps. Precisely, we apply an object-tracking algorithm to the remaining clustered regions (centroids within 1000km). A region at time t2 is considered part of the same heatwave object as a region at t1 if it overlaps by at least 20% of the smaller of the two areas. This overlap threshold is lower than in previous studies (Sánchez-Benítez et al., 2020), which used 50%, but we do not impose additional criteria for significant pattern changes, as in Sánchez-Benítez et al. (2020). Our sensitivity tests show that the results are robust to small variations in the overlap criterion (10-30%, slight variations for 50%), motivating the choice of a smaller threshold. If no overlap is found, the following timestep t3 is tested against t1 to account for single-day gaps in the heatwave object definition.

To handle split and merged events, we implemented a full-history merging approach: any regions that merge or split at any point are assigned a common heatwave object ID throughout their lifetime. While this may produce unusually long heatwave objects, it avoids artefacts due to fluctuations in centroid distances. That is, cases in which centroid distances of different heatwave regions fluctuate close to the threshold. We also tested a proximity criterion by which regions merge or split when the distance between their centroids exceeds a 1000km threshold, but found that the above-mentioned fluctuation issue introduced artificial discontinuities in our identification of heatwave objects. Importantly, our main conclusions remain robust to the choice of tracking method (Supplements S3.2, S3.3).

For each heatwave object, corresponding to a single heatwave ID, we record the centroid and the heatwave object start and end dates, hereafter referred to as the onset and decay. Additionally, we define the peak of the heatwave object as the maximum area-weighted sum of daily maximum temperature anomalies across the heatwave object region. These metrics enable an analysis of the heatwave object life cycle.

To ensure that heatwave objects intersecting the boundaries of the target region are properly tracked, we perform the tracking over an extended domain (35–70°N, 17°W–40°E), including both land and ocean. Next, the results are restricted to the target region by discarding days for which the heatwave object centroid lies outside the target domain.

For the subsequent analysis, a land–sea mask is applied to the heatwave objects. Objects with zero land area at all times are discarded. The onset and decay dates are adjusted to the first and last time steps with non-zero land area. As a result, a given heatwave object may exhibit a temporal gap if it does not intersect land during part of its lifetime.

https://doi.org/10.5194/egusphere-2026-2453
Preprint. Discussion started: 12 June 2026
© Author(s) 2026. CC BY 4.0 License.

2.5 Types of heatwave recurrences

In this study, we take a multi-scale approach to heatwave recurrence, progressing from the local, grid-cell scale to the synoptic scale of heatwave objects and finally to the continental scale. Each scale addresses complementary research questions. The definitions of the three recurrences are schematically illustrated in Figure 1.

2.5.1 Local recurrence

We first examine local (grid-cell) recurrent heatwaves, defined as heatwaves occurring in close succession at the same location, because their impacts on humans, ecosystems, and infrastructure may differ from those of single heatwaves due to the limited recovery time.

Baldwin et al. (2019) define local temporally compound heatwaves as a 3-day temperature exceedance, followed by a 1-day break, and at least a 1-day exceedance thereafter. Similarly, Zhang et al. (2025) require a 3-day exceedance, a maximum 3-day break and another 3-day exceedance. We modify this approach to focus specifically on recurrent heatwaves by requiring that an initial heatwave must be followed by a short break and a subsequent heatwave, rather than a single additional exceedance day. No explicit minimum duration is imposed on either heatwave, as this requirement is already embedded in our grid-cell heatwave definition (minimum duration: 3 days). We set the maximum break duration between heatwaves to 7 days. This longer maximum break criterion, compared with Baldwin et al. (2019), is justified because our heatwave definition already permits a one-day interruption in temperature exceedance. In addition, recovery periods vary widely across systems, such as vegetation or ecosystems, and may extend over several weeks (Sharpe et al., 2019; Sales et al., 2021; Polazzo et al., 2024; Giuliani et al., 2025). Nevertheless, our results remain robust to different maximum break durations (Supplement S3.1).

Note that local recurrent heatwaves may be part of the same heatwave object or belong to different heatwave objects. We treat local recurrent heatwaves equivalently regardless of their heatwave object numbers. Local heatwaves that are neither preceded nor followed by another local heatwave within 7 days are referred to as single heatwaves.

2.5.2 Object recurrence

Because local recurrence can arise from multiple heatwave objects with different physical origins, linking recurrence to the large-scale atmospheric circulation driving heatwaves is challenging at the local scale. We thus complement the local analysis with an object-based approach by classifying heatwave objects according to their degree of local recurrence. Note that such local recurrence must occur within an individual heatwave object and thus represents a subset of the previously identified local recurrences. Specifically, we quantify the fraction of the heatwave object's area that experiences local recurrence at any time during the heatwave object, considering land grid cells only. Then, the upper and lower quartiles of this percentage are determined across the lifetime of the heatwave object, restricting the analysis to heatwave objects with at least one local recurrent heatwave. Heatwave objects above the upper quartile (or below the lower quartile) will hereafter be referred to as strongly (or weakly) recurrent heatwave objects. A sensitivity analysis is provided in Supplement S3.2.

https://doi.org/10.5194/egusphere-2026-2453
Preprint. Discussion started: 12 June 2026
© Author(s) 2026. CC BY 4.0 License.

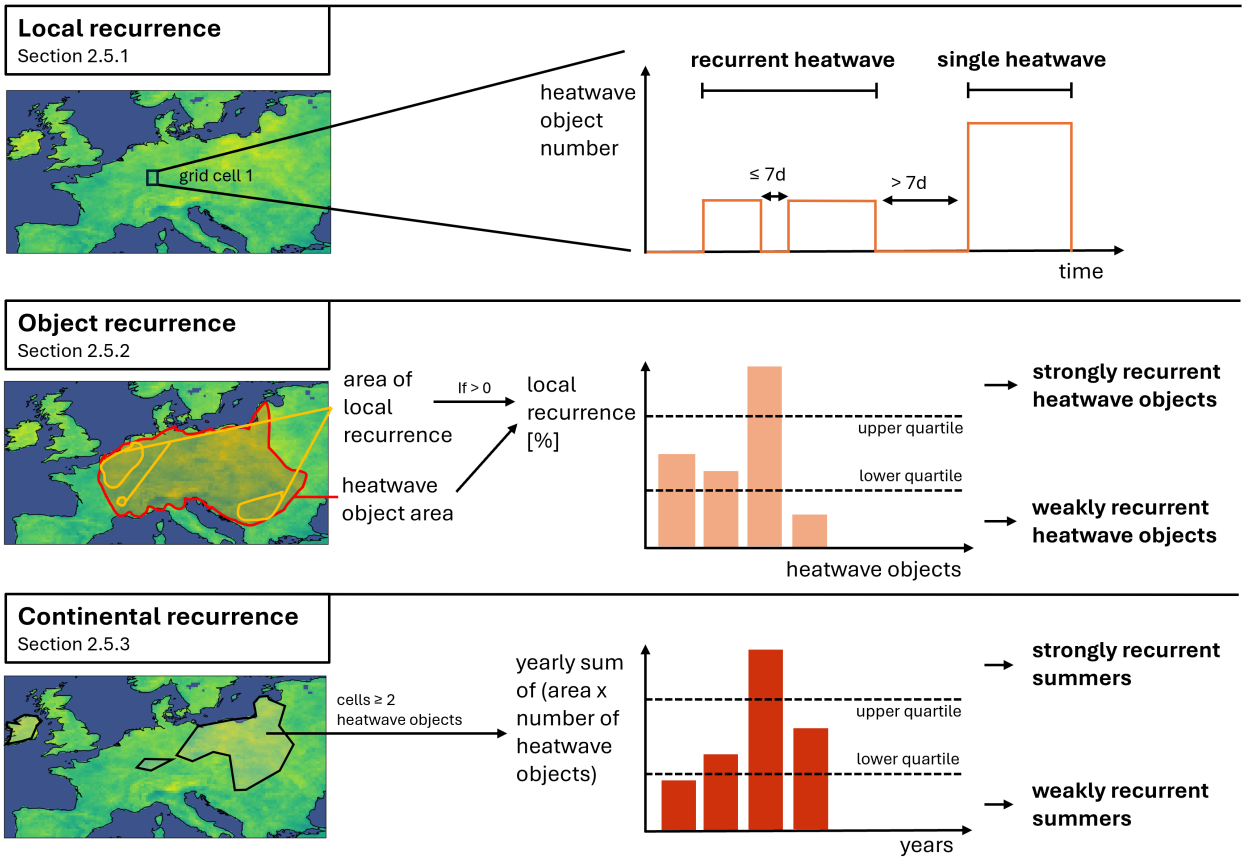

Figure 1. Schematic of the computation of the three recurrence types.

2.5.3 Continental recurrence

While the object recurrence provides a link between local recurrence and large-scale drivers, it does not provide insights into how multiple heatwave objects collectively shape seasonal patterns across the European continent. To address this, we define continental heatwave recurrence by identifying summers in which different heatwave objects repeatedly affect the same locations, regardless of the time interval between them. For instance, one region may experience a heatwave in June and another in August, neither of which must be associated with local or object recurrence. This perspective provides a domain-wide characterization of summers prone to repeated exposure, complementing the local- and object-scale perspectives.

In order to distinguish summers with many heatwave objects, also referred to as strongly recurrent summers, from those with few, we consider only the grid cells that experience at least two different heatwave objects within the May-September period of a single year. For each of these grid cells, the number of distinct heatwave objects affecting it is multiplied by the grid cell area, and the resulting values are summed across all selected grid cells. The final yearly sum is shown in Figure 2. Years

https://doi.org/10.5194/egusphere-2026-2453
Preprint. Discussion started: 12 June 2026
© Author(s) 2026. CC BY 4.0 License.

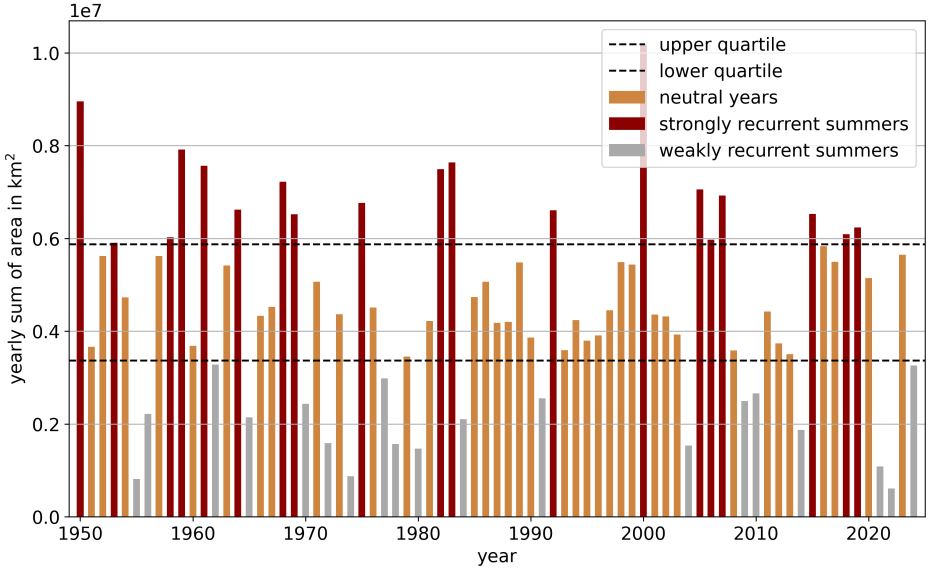

Figure 2. Yearly sum of area-weighted number of heatwave objects per grid cell for grid cells with at least two heatwaves. Colors indicate strongly recurrent summers (red) above the upper quartile, neutral years (orange) in between the quartiles and weakly recurrent summers (grey) below the lower quartile.

exceeding the upper quartile of the yearly sum are classified as strongly recurrent summers (red), while years falling below the lower quartile are defined as weakly recurrent summers (grey). Over the 75-year analysis period, 19 years fall into each of the strongly and weakly recurrent categories, with the remaining 37 years classified as neutral. A sensitivity analysis of the summer-selection procedure is provided in Supplement S3.3.

3 Results

3.1 Local recurrence

In this section, differences in temperature and land-atmosphere anomalies are examined between single and recurrent local heatwaves. Our hypothesis is that such differences may result from soil moisture depletion caused by an initial heatwave, which can amplify temperatures during a subsequent heatwave.

We first analyze daily maximum temperature anomalies, stratified by month (Figure 3a), for single heatwaves, as well as for first and subsequent recurrent heatwaves. Single heatwaves exhibit slightly higher temperature anomalies than recurrent ones in early summer, and values comparable to first events during peak and late summer. Subsequent recurrent heatwaves consistently show similar or lower anomalies than their preceding heatwaves. These results indicate that, at the local scale, following heatwaves are not necessarily hotter than preceding ones, suggesting no temperature amplification in subsequent recurrent heatwaves.

https://doi.org/10.5194/egusphere-2026-2453
Preprint. Discussion started: 12 June 2026
© Author(s) 2026. CC BY 4.0 License.

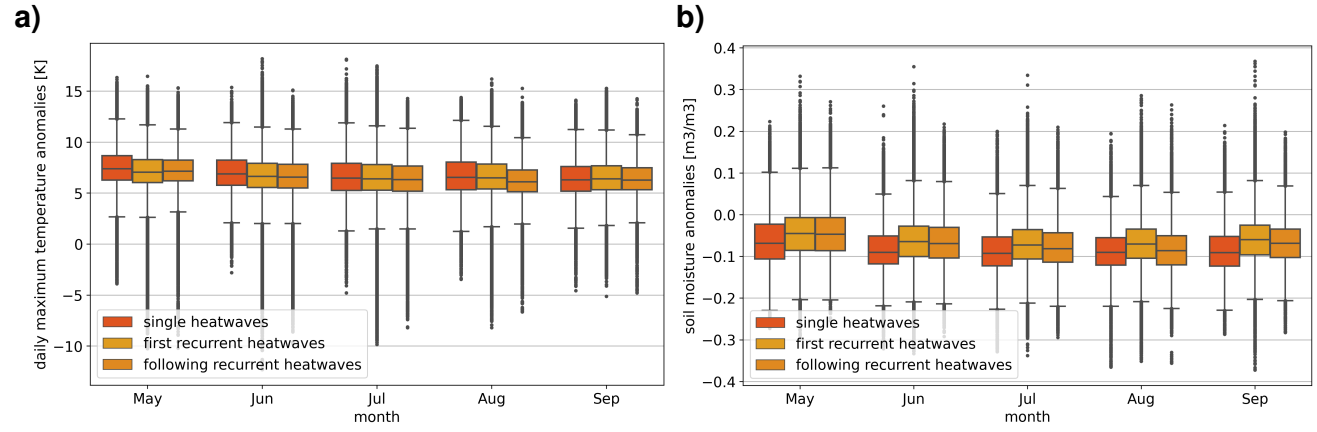

Figure 3. Daily maximum temperature anomalies (a) and soil moisture anomalies in the upper layer (b) during single heatwaves and the first and following local heatwaves in recurrent heatwaves, stratified per month. All local heatwaves are assigned to their start month. Pairwise two-sided Mann–Whitney tests at the 5% level were performed to assess statistically significant differences between distributions of the different event types. All distributions are significantly different except daily maximum temperature and soil moisture between first and subsequent heatwaves during May.

To examine whether this pattern is also reflected in soil moisture, Figure 3b shows the monthly soil moisture anomalies for single and recurrent heatwaves. Throughout the extended summer season, single heatwaves are associated with the greatest soil moisture depletion, in line with their high temperature anomalies. In recurrent heatwaves, the first heatwave shows smaller anomalies, while subsequent ones display comparable (e.g., May) or slightly enhanced depletion (June-September), indicating a subtle preconditioning effect. Interestingly, this accumulation of soil moisture depletion in recurrent heatwaves does not correspond to higher temperatures, in contrast to single heatwaves, where strong drying coincides with the hottest conditions. This suggests that factors beyond local soil moisture shape the temperature anomalies of recurrent heatwaves, whereas single heatwaves demonstrate a more direct soil moisture–temperature feedback.

As heatwave duration may influence the soil moisture depletion and temperature during heatwaves, the monthly mean durations of single, first and subsequent recurrent heatwaves are shown in Table 1, together with their relative proportions. For single heatwaves, mean durations increase by roughly 1 day from May to July, reaching 6.59 days, then declining toward September, reaching a minimum of 4.79 days. First recurrent heatwaves show a similar seasonal pattern, with the shortest durations of around 3 days occurring in September and May, and longer durations during peak summer months. The longest mean durations are observed in August at 7.5 days, while July values are lower than those in June and August. Subsequent recurrent heatwaves have the shortest durations in May and June, around 3 days, with increasing durations later in the summer. The highest mean duration and variability occur in July, at 6.69 days. Unlike the other two classes, September recurrent heatwaves display the second-highest durations, at 5.6 days, highlighting a distinct seasonal behavior. Overall, mean durations of recurrent heatwaves have stronger seasonal fluctuations, varying by about 4 days for first and 3 days for following heatwaves, compared to the roughly 1-day variation in single heatwaves. Standard deviations generally range between 1 and 3 days, with

https://doi.org/10.5194/egusphere-2026-2453
Preprint. Discussion started: 12 June 2026
© Author(s) 2026. CC BY 4.0 License.

Table 1. Monthly durations and proportions of single, first and following recurrent local heatwaves during May to September.

	heatwave type	May	Jun	Jul	Aug	Sep
duration [d]	single	5.64 ± 1.48	5.85 ± 2.18	6.59 ± 2.85	6.34 ± 2.50	4.79 ± 1.33
(mean ± std)	first	3.33 ± 0.82	6.02 ± 3.06	4.63 ± 1.83	7.51 ± 2.63	2.86 ± 1.03
	following	3.17 ± 0.41	3.25 ± 1.05	6.69 ± 4.42	4.22 ± 2.44	5.60 ± 2.97
proportion	single	75.0	75.3	72.3	71.0	78.5
of events [%]	first	13.3	11.9	13.6	12.8	7.2
	following	11.7	12.8	14.1	16.2	14.3

lower values for recurrent heatwaves in May and a notably high variability of 4.4 days for the following recurrent heatwaves in July. Considering soil moisture anomalies, higher depletion in following heatwaves compared to first ones does not clearly correspond to longer or shorter durations. Likewise, variations in duration of first or following heatwaves are not reflected in the magnitude of temperature anomalies.

We further examine whether the relative frequency of different heatwave types may explain some of the above results (Table 1). The data show that the majority of local heatwaves occur as single heatwaves. Recurrent local heatwaves account for 21.5% to 29.0% of all local heatwave days, with the highest proportions in July and August and the lowest in September. Except for May, each month exhibits a higher number of following recurrent heatwave days than first recurrent heatwaves. Over the extended summer months, this difference increases. Correspondingly, the soil moisture and temperature anomalies of following heatwaves tend to diverge more from those of the first heatwaves throughout the extended summer, except in September.

Therefore, the number of recurrent heatwave days may influence the observed temperature and soil moisture anomalies, whereas no systematic relationship with heatwave duration is evident. Importantly, the results presented in this section remain qualitatively consistent across different maximum break lengths between local recurrent heatwaves (Supplement S3.1). To further explore the mechanisms underlying local recurrence, we examine a larger scale where heatwaves form spatiotemporally coherent objects and therefore may be more easily linked to the large-scale atmospheric circulation.

3.2 Object recurrence

In the object-based perspective, we define heatwave objects with substantial fractions of locally recurrent grid cells as strongly recurrent heatwaves. In total, 34.5% of all heatwave objects exhibit local recurrence. By conditioning on the fraction of the object area affected by local recurrence, we explicitly link local recurrence with synoptic-scale coherence, which cannot be resolved at the purely local scale. Precisely, heatwave objects with a local recurrence fraction above 17.4% (upper quartile) or below 1.8% (lower quartile) are selected, among those containing at least one local recurrent heatwave. This restriction ensures that only objects of sufficient duration to permit local recurrence are considered.

The selected strongly and weakly recurrent heatwave objects differ in their temporal and spatial characteristics. Strongly recurrent heatwave objects have longer mean durations (27.91 days) than weakly recurrent ones (8.58 days), indicating that longer-lasting objects are more likely to shift spatially and subsequently return to some of the previously affected regions,

https://doi.org/10.5194/egusphere-2026-2453
Preprint. Discussion started: 12 June 2026
© Author(s) 2026. CC BY 4.0 License.

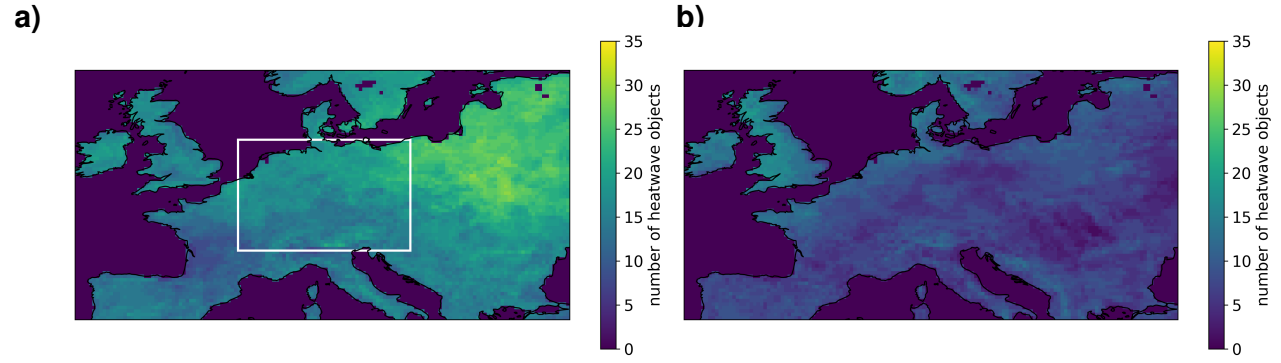

Figure 4. Spatial distribution of strongly (a) and weakly (b) recurrent heatwaves. Shown is the total number of different heatwave objects per grid cell. (a) Example of a 1000 × 1000 km box (white) illustrating the considered spatial extent for centered composites (e.g. Figure 5).

thereby generating local recurrences. This hypothesis is further supported by their size, with strongly recurrent objects covering a larger mean spatial extent ($2.6{*}10^6$ km^2) than weakly recurrent ones ($0.9{*}10^6$ km^2). In addition, the spatial distributions of strongly and weakly recurrent heatwaves are compared in Figure 4a and b, respectively. The cumulative number of heatwave objects affecting each grid cell is higher for strongly recurrent heatwaves, reflecting their larger spatial extent. Strongly recurrent heatwaves occur most frequently in north-eastern Central Europe, whereas weakly recurrent heatwaves are more common in northwestern regions. This pattern is consistent with the predominance of local heatwave recurrence in north-eastern Central Europe (Supplementary Figure S2).

Building on this spatial perspective, Figure 5 presents centered composites of the average daily maximum temperature (a-c) and upper-layer soil moisture (d-f) anomalies for both strongly (left) and weakly (middle) recurrent heatwave objects, along with their difference (right). Soil moisture depletion is significantly stronger during strongly recurrent heatwave objects, extending around the centroid and particularly toward the north-eastern sector. Moreover, depletion is more widespread than in weakly recurrent heatwave objects, particularly northwest and southwest of the centroid. This may be influenced by the presence of ocean grid cells, reducing data coverage. Consistent with these soil moisture anomalies, daily maximum temperature anomalies are up to 1°C higher, especially northeast of the centroid. This may be related to the longer duration of strongly recurrent heatwave objects. In addition, similar to the soil moisture depletion, these higher temperature anomalies extend over a larger area during strongly recurrent heatwave objects, notably toward the northwest and southwest, in line with the generally larger continental area affected by these events. Thus, heatwave objects with a large fraction of local recurrence are characterized by higher and more widespread soil moisture depletion and temperature anomalies compared to weakly recurrent ones.

The apparent decoupling between soil moisture and temperature for recurrent local heatwaves is not present for strongly recurrent heatwave objects. We hypothesize that local recurrences may occur more frequently at the edges of heatwave objects, where small spatial shifts, reversed a few days later, enable local recurrence. Closer to the heatwave object centroid, single local heatwaves are likely to prevail, as local recurrence would require larger spatial shifts. Therefore, the generally smaller soil

https://doi.org/10.5194/egusphere-2026-2453
Preprint. Discussion started: 12 June 2026
© Author(s) 2026. CC BY 4.0 License.

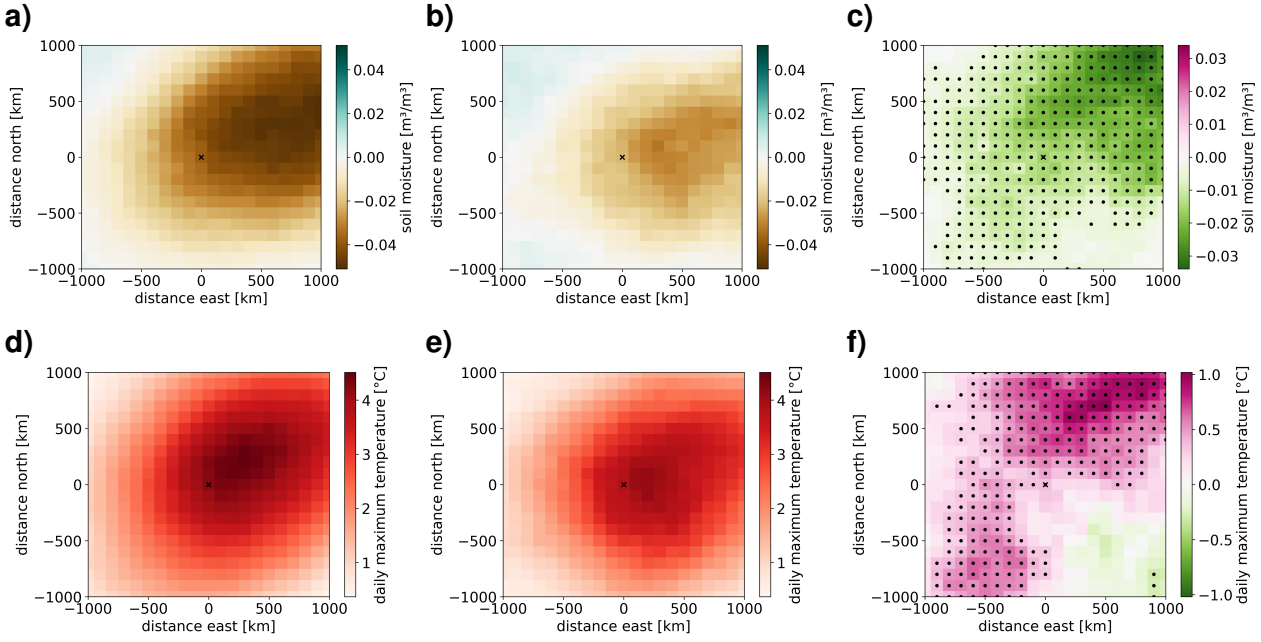

Figure 5. Centered composites showing the difference (right) between strongly (left) and weakly (middle) recurrent heatwaves in soil moisture anomalies in the upper soil layer (a-c) and detrended daily maximum temperature anomalies (d-f). Data is averaged for all heatwaves, with the composites centered on the heatwave centroid and the data composited relative to the distance to it. Dots represent statistically significant differences between strongly and weakly recurrent heatwaves based on a t-test at the 5% significance level following an FDR correction.

moisture and temperature anomalies at the edges, compared to the center of the heatwave object, may explain the decoupling between temperature and soil moisture for local recurrence.

In addition to soil moisture and temperature, the object recurrence perspective enables the investigation of atmospheric circulation patterns associated with strongly and weakly recurrent objects. Figure 6 shows the monthly frequency of weather regimes (see Supplement S1 for spatial clusters) for all heatwave object days, as well as for days associated with strongly and weakly recurrent heatwave objects. This represents the most parameter-sensitive aspect of our study, as regime frequencies can shift slightly depending on the tracking algorithm and the duration of local recurrence breaks, which may alter heatwave object size or local recurrence fractions and thus affect event selection. For this reason, we focus only on the patterns in Figure 6, which we have found to be robust to small parameter changes.

In the weather regime framework that we adopt, atmospheric blockings are captured by three blocked regimes: Greenland, European, and Scandinavian Blocking. Overall, strongly recurrent heatwaves occur less frequently during Greenland Blocking (GL) than weakly recurrent ones, which is robust for the peak summer months June, July and August. This difference may partly reflect that strongly recurrent heatwaves occur more frequently at higher latitudes, where GL is associated with a low pressure anomaly and thus negative temperature anomalies. In contrast, European Blocking (EuBL) becomes more prominent

https://doi.org/10.5194/egusphere-2026-2453
Preprint. Discussion started: 12 June 2026
© Author(s) 2026. CC BY 4.0 License.

for strongly recurrent heatwaves in July and August, whereas it is less frequent in May and has the tendency to be less frequent in September compared with weakly recurrent events. Scandinavian Blocking (ScBL) shows a different seasonal structure, occurring robustly more frequently in July and less frequently in August. The contrasting seasonal patterns of the blocked weather regime underscore the importance of analyzing summer months individually, as well as the added value of considering a seven-regime classification as opposed to the canonical four-regime approach.

In addition to the blocked regimes, four cyclonic regimes are distinguished, which are more transient. The Atlantic Trough (AT) occurs more frequently for strongly compared to weakly recurrent heatwaves in early summer (May and June), while the Zonal Regime (ZO) is less frequent in September. Atlantic Ridge (AR) is less frequent during strongly recurrent heatwaves in July, while the Scandinavian Trough (ScTr) tends to be more frequent in September.

In summary, strongly recurrent heatwaves occur less frequently under Greenland blocking, but more frequently under European blocking during the peak summer months, and more frequently under Scandinavian blocking in July, but less frequently in August. As blockings are typically more persistent than transient regimes, and the longest heatwave durations are reached in July (Supplement S1), this behavior may explain the longer heatwave durations for strongly recurrent heatwaves.

3.3 Continental recurrence

We next consider the recurrence of multiple heatwave objects within a single summer to assess continental-scale seasonal recurrence. The continental definition of recurrence, based on the number of heatwave objects and the affected area, allows for two types of strongly recurrent summer seasons. One possibility is a high number of heatwave objects occurring within a relatively small region, while the other consists of a smaller number of heatwave objects affecting a large region. Both patterns are equally captured under the continental definition of a strongly recurrent summer season.

However, since a strongly recurrent summer may also include a larger total number of heatwaves than a weakly recurrent summer, this raises the question of whether strongly recurrent summers merely correspond to the hottest summers or whether heatwave recurrence represents a distinct characteristic. Figure 7 addresses this aspect by presenting the yearly detrended daily maximum temperature anomalies, colored according to the classification of weakly and strongly recurrent summers.

Visual inspection reveals a substantial overlap between strongly recurrent summers and the hottest summers (defined as years with temperature anomalies above the upper quartile), as well as between weakly recurrent summers and the coldest summers (below the lower quartile). However, the two classifications are not identical. Of the 19 strongly recurrent summers, 11 belong to the hottest category, corresponding to 57.89 %, while the remaining summers fall into the neutral category. Conversely, 13 out of 19 weakly recurrent summers occur during the coldest summers, corresponding to an overlap of 68.42 % and none are among the hottest summers. Notably, several highly anomalous summers in terms of temperature, such as 2003 and 1996, are not exceptional with respect to recurrence. Summer temperature anomalies and recurrence are thus related but not interchangeable.

Figure 8 provides an overview of heatwave characteristics across the summer months for strongly and weakly recurrent summers, establishing a baseline for subsequent analyses. Strongly recurrent summers exhibit a higher total number of heat-

https://doi.org/10.5194/egusphere-2026-2453
Preprint. Discussion started: 12 June 2026
© Author(s) 2026. CC BY 4.0 License.

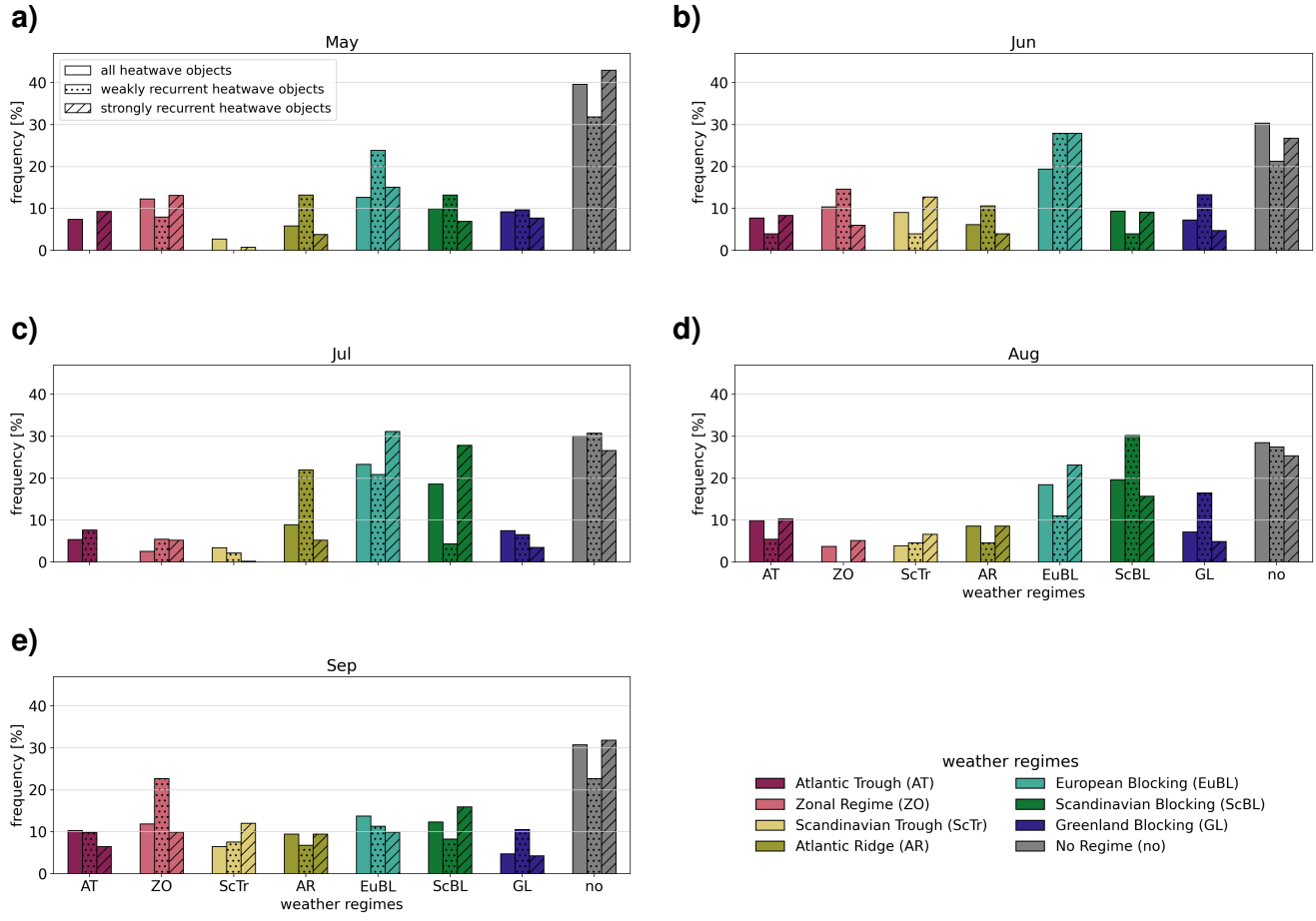

Figure 6. Monthly weather regime frequencies for all, weakly recurrent, and strongly recurrent heatwave days. No hatching: all heatwaves; dotted: weakly recurrent; striped: strongly recurrent. The spatial weather regime clusters are illustrated in Supplementary Figure S1.

wave objects than in weakly recurrent summers, particularly in July (Figure 8a). In both cases, the total number of heatwave objects is lowest in September, and differences in object numbers during May and September are comparable to those in the other months. To account for differences in heatwave object duration, Figure 8b presents the number of heat days per month. The largest difference occurs in May, followed by July and September. Notably, although the number of heatwave objects in strongly recurrent summers is not substantially higher in May or September, these summers experience considerably more heat days in May and September. This pattern suggests that heatwave objects in May and September may be longer or begin earlier in May and later in September in strongly recurrent summers, highlighting the role of transition months in shaping summer heatwave dynamics. Analysis of heatwave object duration (Figure 8c) shows a slightly higher median duration in strongly recurrent summers, although weakly recurrent summers exhibit a few exceptionally long heatwave objects. In addition, the

https://doi.org/10.5194/egusphere-2026-2453
Preprint. Discussion started: 12 June 2026
© Author(s) 2026. CC BY 4.0 License.

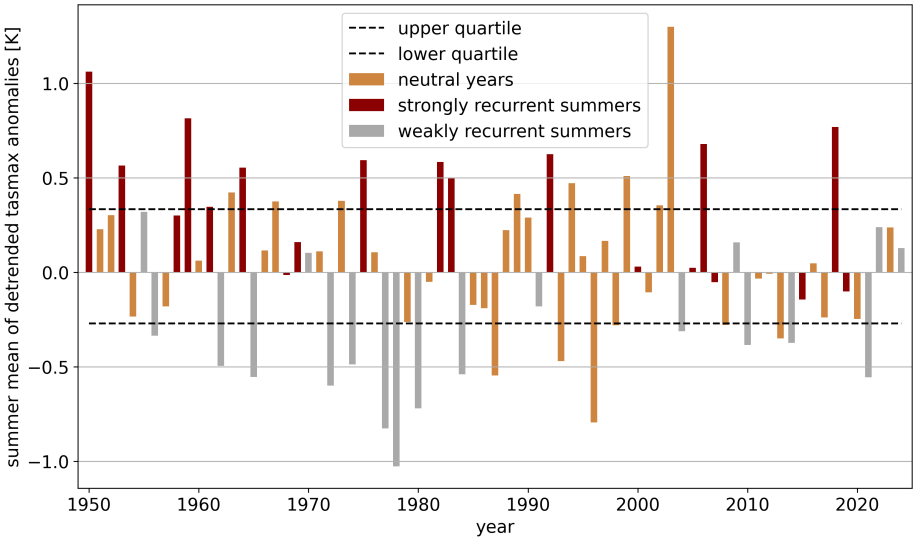

Figure 7. Yearly detrended daily maximum temperature anomalies averaged over the extended summer months. Red indicates strongly recurrent summers, grey weakly recurrent summers, and orange years which lie in between. The dashed lines represent the upper and lower quartiles of detrended daily maximum temperature anomalies, as an indication of hot and cold years.

median area affected by heatwave objects in strongly recurrent years is almost 135,000 km^2 larger than in weakly recurrent years (Figure 8d).

Overall, these results indicate that strongly recurrent summers are characterized by a higher number of heatwave objects with slightly longer durations affecting larger areas, potentially increasing spatial overlap between heatwave objects. Although the monthly occurrence of heatwave objects is similar across the two classes, the higher number of heat days in May and September suggests a prolonged heatwave season for strongly recurrent summers.

Given that strongly recurrent summers feature a higher number of heat days while not being uniformly hotter, we further examine the temperature characteristics of heatwave objects in strongly and weakly recurrent summers. To this end, averages of detrended, deseasonalized daily maximum temperatures were calculated around the heatwave object centroids separately for the two classes. The differences between objects in strongly and weakly recurrent summers at the onset, peak, and decay phases are shown in Figure 9 (top). At the heatwave object onset, there is no significant temperature difference between the two types of summers. During the peak phase, however, strongly recurrent summers exhibit significantly higher temperatures (approximately +2.5K), particularly northwest of the heatwave object centroid. Finally, temperature differences are no longer significant during decay, yet a slight residual warming remains around the centroid. Therefore, similar to object recurrence, daily maximum temperatures are higher during heatwave objects in summers with a high continental recurrence.

As land-atmosphere interactions modulate heatwave temperatures, soil moisture anomalies in the upper soil layer are also analyzed (Figure 9 bottom). Overall, heatwave objects in strongly recurrent summers exhibit statistically significant lower soil

https://doi.org/10.5194/egusphere-2026-2453
Preprint. Discussion started: 12 June 2026
© Author(s) 2026. CC BY 4.0 License.

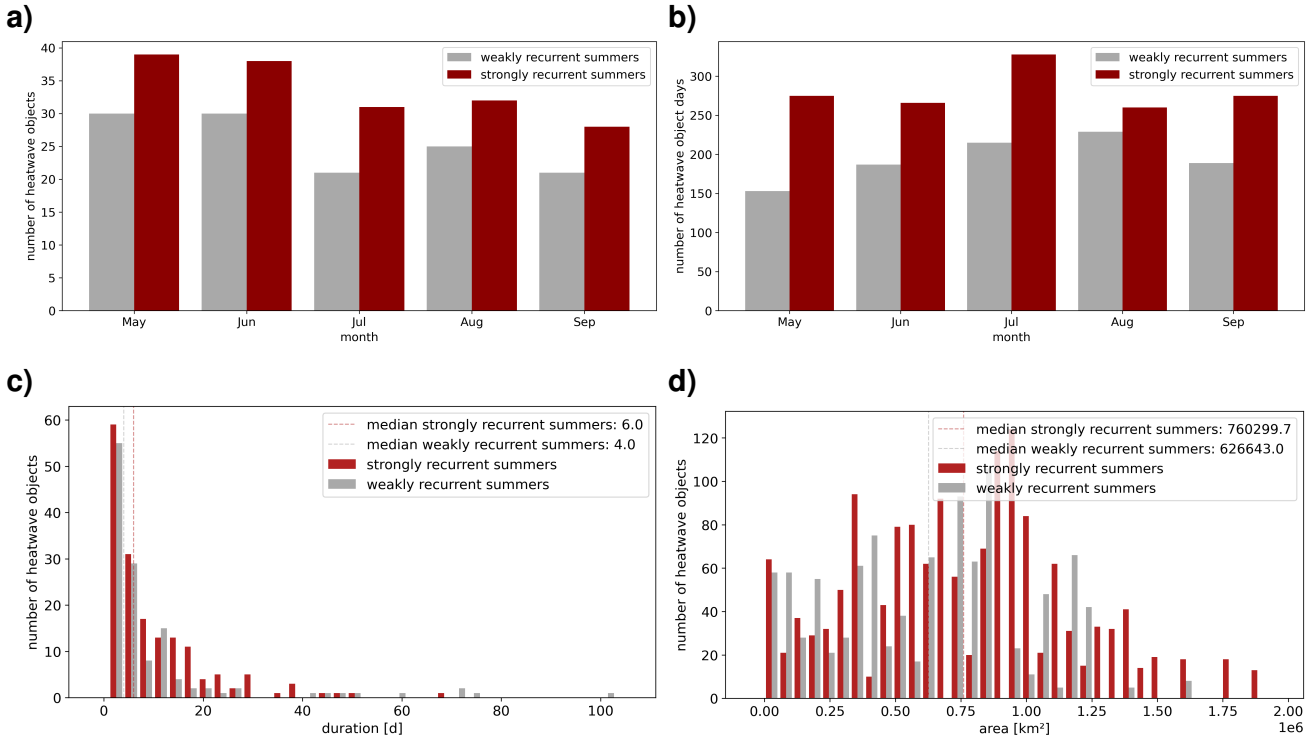

Figure 8. Basic statistics for strongly and weakly recurrent summers. (a) monthly number of heatwaves (with each heatwave assigned to the month with the higher number of object heat days, if equal to the start month), (b) monthly number of heat days, (c) duration and (d) area histogram of heatwave objects for all months with dashed lines indicating the median for both types of summer.

moisture than those in weakly recurrent summers during onset, peak, and decay phases. The difference between the summer types is largest during the peak phase, followed by decay and onset. During the onset and decay phases, the largest differences occur northeast of the heatwave object centroid. The spatial pattern during the peak phase is similar to that of the temperature anomalies at peak, but is shifted slightly eastward.

We conclude that heatwave objects in strongly recurrent summers are characterized by higher peak temperatures, likely amplified by greater soil moisture depletion. Soils are already modestly depleted at heatwave object onset in these summers, indicating a distinct preconditioning compared to weakly recurrent years. The heatwave objects themselves further reduce soil moisture more strongly in strongly recurrent summers, with differences during the decay phase being more pronounced relative to onset.

Given that soil moisture anomalies already differ at heatwave object onset between strongly and weakly recurrent summers, monthly soil moisture anomalies are analyzed as centered composites to assess the seasonal evolution (Figure 10). In both summer types, soil moisture depletion occurs around the heatwave object centroid throughout the season, with the strongest anomalies generally located northeast of the centroid. Depletion is consistently and statistically significantly greater in strongly

https://doi.org/10.5194/egusphere-2026-2453
Preprint. Discussion started: 12 June 2026
© Author(s) 2026. CC BY 4.0 License.

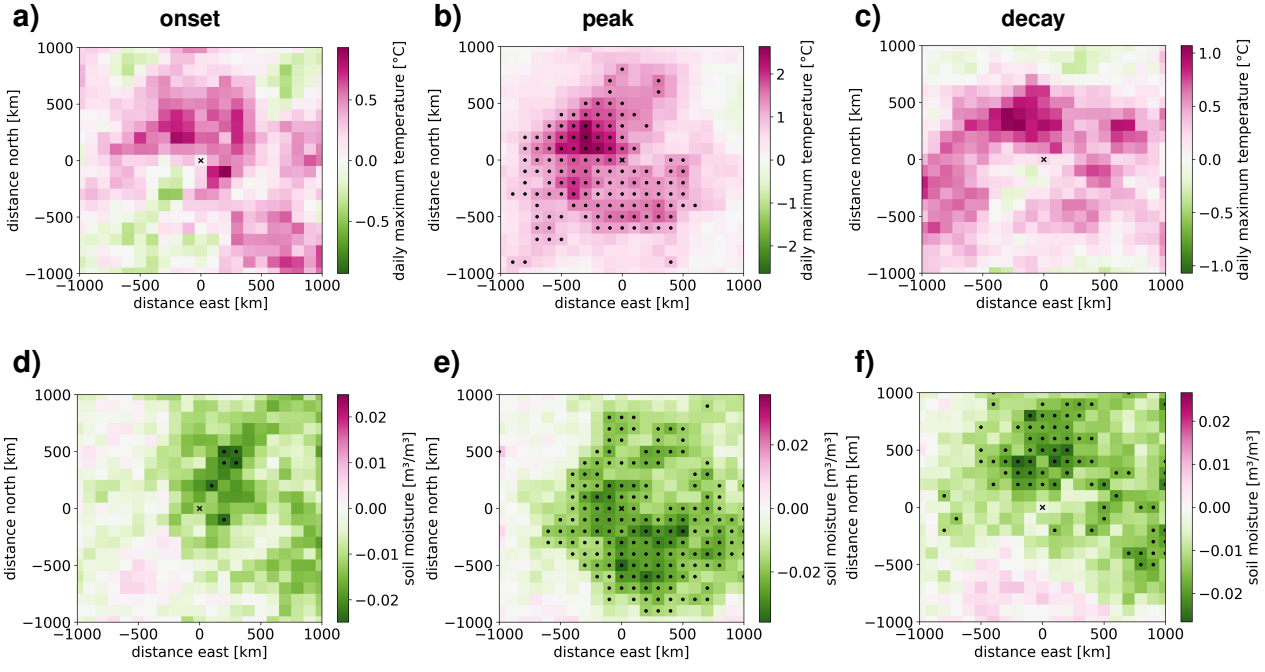

Figure 9. Centered composites showing the difference between strongly and weakly recurrent summers in detrended daily maximum temperature anomalies (a-c) and soil moisture anomalies in the upper soil layer (d-f) for the heatwave onset (left), peak (middle), and decay (right). Data is averaged for all heatwaves, with the composites centred on the heatwave centroid and the data composited relative to the distance to it. Dots represent statistically significant differences between strongly and weakly recurrent summers based on a t-test at the 5% significance level following an FDR correction.

recurrent summers, particularly in the vicinity of the centroid. From May through July, the spatial extent of depletion is larger in these summers, whereas in late summer, heatwave objects become more localized. In weakly recurrent summers, maximum depletion is reached in July, with lower anomalies persisting into August and September, whereas in strongly recurrent summers, maximum anomalies decrease only marginally by September. Collectively, these results indicate that soil moisture depletion during heatwave objects in strongly recurrent summers is already more pronounced and widespread in early summer, and elevated anomalies persist throughout the season compared to weakly recurrent summers.

https://doi.org/10.5194/egusphere-2026-2453
Preprint. Discussion started: 12 June 2026
© Author(s) 2026. CC BY 4.0 License.

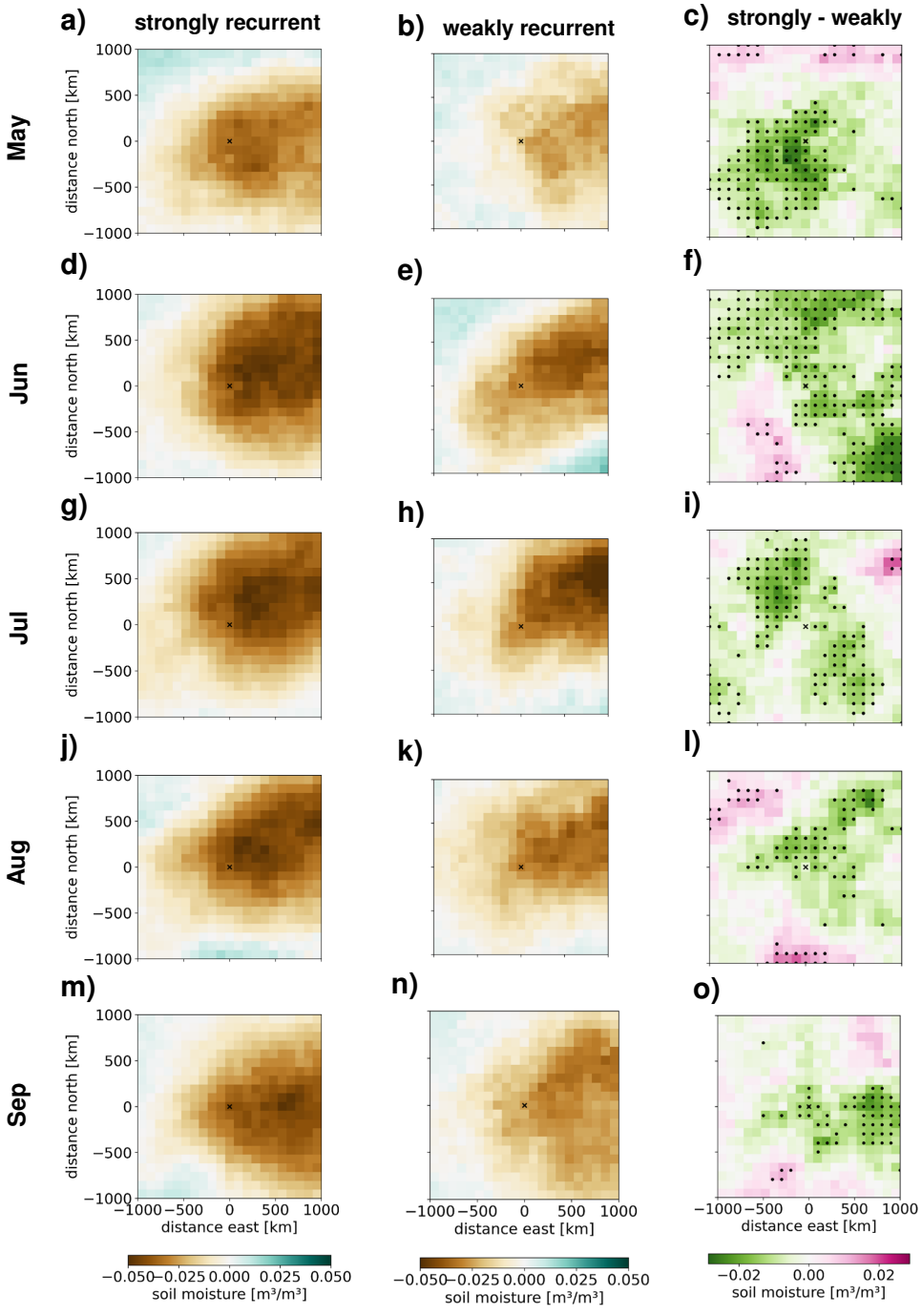

Figure 10. Centered composites showing soil moisture anomalies in the upper soil layer relative to the heatwave centroid split into the months May to September (rows). The left column corresponds to heatwaves in strongly compound summers, the middle column to heatwaves in weakly compound summers and the right column to the difference between them. Data is averaged for all heatwaves, with the heatwave centroid in the center and the data aligned and averaged relative to the distance to it. Dots represent statistically significant differences between strongly and weakly recurrent summers based on a t-test and FDR correction.

https://doi.org/10.5194/egusphere-2026-2453
Preprint. Discussion started: 12 June 2026
© Author(s) 2026. CC BY 4.0 License.

In summary, continental heatwave recurrence represents a distinct feature of summer rather than merely reflecting particularly hot seasons. Strongly recurrent summers are characterized by a greater number of heat days, larger affected areas, higher daily maximum temperatures during heatwave objects, and more pronounced soil moisture depletion throughout the extended summer period. As continental recurrence does not impose a maximum break duration between two heatwave objects, the question arises whether continental recurrence is linked to local recurrence or if the two represent complementary but independent aspects of heatwave recurrence.

3.3.1 Link to local recurrence

To investigate the relationship between continental and local heatwave recurrence, the area-weighted sum of local recurrences (as previously defined as heatwaves separated by maximum 7 days) is illustrated in Figure 11, colored according to the continental recurrence definition. Local recurrent heatwaves occur every summer. Summers with high local recurrence (above the upper quartile) encompass 10 (52.63%) strongly recurrent, 6 (31.58%) neutral and 3 weakly recurrent summers (15.79%). In contrast, summers with little local recurrence (below the lower quartile) comprise 10 (52.63%) weakly recurrent, 7 (36.84%) neutral and 2 (10.53%) strongly recurrent summers. Therefore, local recurrence predominantly occurs in strongly recurrent summers and is less frequent in weakly recurrent ones, indicating a relationship between local and continental recurrence. However, a strongly recurrent summer does not necessarily imply a high number of local recurrent heatwaves, highlighting that the two approaches capture distinct, complementary aspects of heatwave recurrence at different spatial scales.

4 Summary and discussion

In this study, we investigated heatwave recurrence across Europe at multiple spatial scales. At the local scale, we analyzed soil moisture and temperature anomalies associated with recurrent heatwaves, defined as repeated heatwaves separated by short breaks at a fixed location. To link local recurrence to larger, coherent structures, we then examined heatwave objects exhibiting strong and weak local recurrence. Their relationship with the large-scale atmospheric circulation, temperature and soil moisture anomalies was analyzed. Finally, at the continental scale, we explored the recurrence of multiple heatwave objects across Central Europe within a summer season and assessed how these patterns relate to local heatwave recurrence. This multi-scale approach to heatwave recurrence captures how phenomena at different spatial scales collectively influence the characteristics of heat extremes across Europe. The main findings, framed by our research questions, are as follows:

- *How do locally recurrent heatwaves differ from isolated heatwaves in terms of temperature and soil-moisture anomalies?* Local recurrent heatwaves generally display weaker daily maximum temperature and soil moisture anomalies than single events, though subsequent recurrent heatwaves show stronger negative soil moisture anomalies than the first heatwaves (except May). No systematic link with heatwave duration is observed. However, as the proportion of subsequent recurrent heatwaves increases and peaks in August, soil moisture and temperature anomalies increasingly diverge from those of the first recurrent events. Overall, recurrent local heatwaves account for 21.5% to 29.0% of all local heatwaves, peaking in July-August and reaching a minimum in September.

https://doi.org/10.5194/egusphere-2026-2453
Preprint. Discussion started: 12 June 2026
© Author(s) 2026. CC BY 4.0 License.

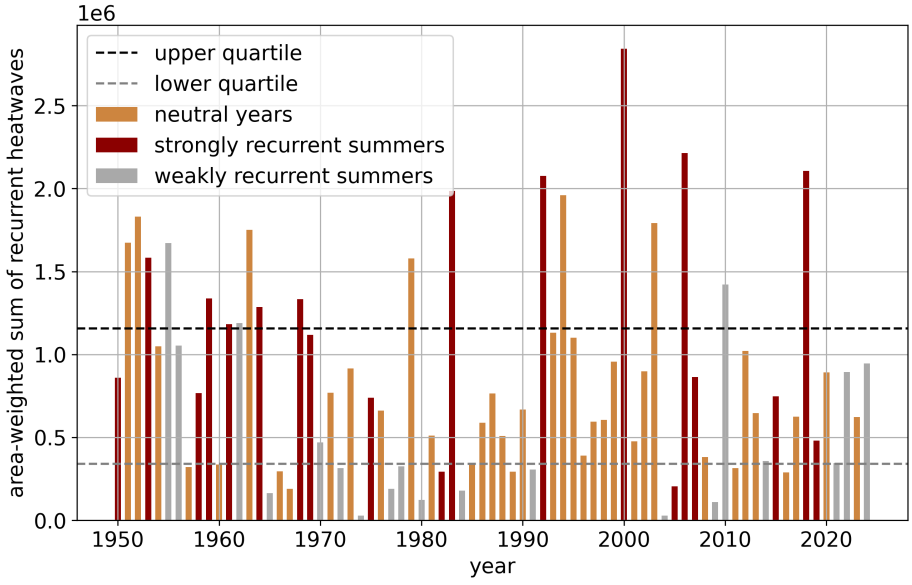

Figure 11. Area-weighted sum of number of local recurrences per year. Red colors indicate strongly recurrent summers, grey weakly recurrent summers, and orange neutral summers. Dashed lines indicate the 25th and 75th percentiles of the local recurrence sum.

– *Which physical characteristics and atmospheric circulation patterns distinguish heatwave objects with strong versus weak local recurrence?*

Heatwave objects with substantial local recurrence last longer, cover a larger region, and are associated with higher soil moisture and daily maximum temperature anomalies. The northeastern part of the analysis domain, corresponding to the Baltic states, Belarus, and eastern Poland, experiences a higher incidence of strongly recurrent heatwave objects, in line with the spatial distribution of local recurrences. Further, the objects recur more frequently under European Blocking in July and August, and under Scandinavian Blocking in July, while they recur less frequently under Scandinavian Blocking in August and Greenland Blocking in the peak summer months.

– *How does the recurrence of heatwave objects within a summer shape their characteristics across Europe, and how does continental-scale recurrence relate to local heatwave recurrence?*

While roughly two-thirds of strongly (weakly) recurrent summers coincide with hot (cold) conditions, exceptional temperature anomalies and heatwave object recurrence are not equivalent, demonstrating that recurrence represents a distinct facet of summer heat extremes. Further, strongly recurrent summers experience slightly more heatwave objects compared to weakly recurrent ones, particularly in July, and notably more heat days in May and September. Heatwave object-affected areas are larger and daily maximum temperature anomalies are higher, although durations are only slightly longer. Soil moisture depletion during heatwave objects in strongly recurrent summers is more pronounced through-

https://doi.org/10.5194/egusphere-2026-2453
Preprint. Discussion started: 12 June 2026
© Author(s) 2026. CC BY 4.0 License.

out the summer season, more widespread in early summer, and shows a slight eastward shift relative to temperature anomalies. The approximately 50% overlap between strongly recurrent summers and those exhibiting high local recurrence highlights that continental and local recurrence are complementary yet distinct dimensions of heatwave recurrence, despite their partial interrelation.

This study provides a novel perspective on heatwave recurrence by examining it across multiple spatial scales. Our approach enables the connection between local recurrent heatwaves and larger-scale structures, such as the large-scale atmospheric circulation. It demonstrates how recurrence manifests differently at local, object, and continental scales, and how interactions across larger regions influence the characteristics of recurrent heatwaves. To our knowledge, no prior study has investigated heatwave recurrence across multiple spatial scales, nor heatwave objects with varying levels of local recurrence or recurrence at the continental scale within a summer season.

Previous studies, such as Baldwin et al. (2019) and Zhang et al. (2025), have investigated recurrent or so-called temporally compound heatwaves at the grid-cell scale globally and over China, respectively. Both show a trend in more recurrent heatwaves in a warming climate. Their definition of temporally compound heatwaves is conceptually similar to ours, with small variations in the exact duration thresholds. Zhang et al. (2025) show that the increasing trend in compound heat events results in greater heat stress compared to single events, mainly due to prolonged sequences of extreme hot days. Consistently, our results indicate that locally recurrent heatwaves are not systematically hotter than single events. We hypothesize that lower soil moisture depletion and milder temperatures during local recurrent heatwaves may result from their spatial position relative to heatwave objects. For a local recurrence to occur, a heatwave object must cease and then return to the same region. Consequently, local recurrences may occur near the edges of heatwave objects, thus experiencing lower peak temperatures. Breaks between local recurrences may be associated with troughs and precipitation, which could explain the reduced soil moisture depletion compared to single heatwaves. However, our study did not explicitly test this hypothesis, leaving the precise mechanisms underlying these patterns as open questions for future research.

While providing a novel perspective on heatwave recurrence, this study has several limitations and opens opportunities for future work. The heatwave definition and recurrence metrics are relatively complex and, to date, are not directly comparable with other studies, given the lack of multi-scale analyses. Therefore, we do not claim these definitions are optimal; however, sensitivity tests confirm that the results are robust to parameter choices. The primary aim was to introduce a unified multi-scale framework and examine differences between recurrent and non recurrent heatwaves at different scales. Therefore, our methodology does not explicitly address causal mechanisms, and the precise relationships between soil moisture, atmospheric circulation, and other potential drivers remain to be investigated. Further, our analysis is limited to heatwave hazards. A more complete assessment of heatwave risks, including exposure and vulnerabilities would provide insight in support of mitigation and adaptation strategies. Extending this analysis to other regions globally could further clarify the generality of the observed patterns.

As shown by Hundhausen et al. (2023), increasing global warming may extend the heatwave season in Central Europe to October, thereby increasing the potential for longer sequences of recurrent heatwaves across multiple spatial scales. In parallel, locally temporally compound heatwaves are projected to become more frequent under a warming climate (Baldwin et al., 2019;

https://doi.org/10.5194/egusphere-2026-2453
Preprint. Discussion started: 12 June 2026
© Author(s) 2026. CC BY 4.0 License.

Zhang et al., 2025), emphasizing the need to better understand their underlying mechanisms. The multi-spatial-scale framework that we present in this study serves as a basis for future investigations into the processes underlying recurrent heatwaves.

https://doi.org/10.5194/egusphere-2026-2453
Preprint. Discussion started: 12 June 2026
© Author(s) 2026. CC BY 4.0 License.

Data availability. The ERA5 reanalysis data can be downloaded from https://doi.org/10.24381/cds.adbb2d47 (Hersbach et al., 2023). The weather regime classification is available through Grams (2026).

Author contributions. ID, GM, AL and JGP designed the study. ID performed the data analysis and wrote the first draft of the manuscript. ID created the figures. SB contributed with methodology. All authors discussed the results and contributed with manuscript revision.

Competing interests. The authors have no competing interest to declare.

Acknowledgements. The research leading to these results has been done in the scope of the ClimXtreme2 project (www.climxtreme.de), particularly within subproject *B3.7 Dynamical Systems perspective on weather regimes and heatwaves in a changing climate* (01LP2323N ,01LP2323A, 01LP2322A). ClimXtreme2 is funded by the German Federal Ministry of Research, Technology and Space (BMFTR) within the framework of "Research for Sustainable Development" (FONA). The analysis was carried out on the supercomputer Levante at DKRZ, Hamburg, and datasets provided by DKRZ via the DKRZ data pool were used. This work used resources of the Deutsches Klimarechenzentrum (DKRZ) granted by its Scientific Steering CommTempee (WLA) under Project IDs bm1159 and bb1152. In some instances, ChatGPT was used to rephrase sentences for clarity. JGP thanks the AXA research fund for support. GM acknolwedges support from the Swedish Research Council Vetenskapsrådet (grant no. 2022-06599), the Swedish Research Council FORMAS (grant no. 2022-01845) and the European Union Horizon Europe research and innovation programme (ClimTip, grant agreement no. 101137601). ID thanks the Graduate School for Climate and Environment (GRACE) of the Karlsruhe Institute of Technology for the funding of the research stay at Uppsala University. ID thanks GM and the researchers at the Swedish Centre for Impacts of Climate Extremes for fruitful discussions during the research stay at Uppsala University.

https://doi.org/10.5194/egusphere-2026-2453
Preprint. Discussion started: 12 June 2026
© Author(s) 2026. CC BY 4.0 License.

References

Baldwin, J. W., Dessy, J. B., Vecchi, G. A., and Oppenheimer, M.: Temporally Compound Heat Wave Events and Global Warming: An Emerging Hazard, Earth's Future, 7, 411–427, https://doi.org/10.1029/2018EF000989, 2019.

Barriopedro, D., García-Herrera, R., Ordóñez, C., Miralles, D. G., and Salcedo-Sanz, S.: Heat Waves: Physical Understanding and Scientific Challenges, Reviews of Geophysics, 61, e2022RG000 780, https://doi.org/10.1029/2022RG000780, 2023.

Becker, F. N., Fink, A. H., Bissolli, P., and Pinto, J. G.: Towards a more comprehensive assessment of the intensity of historical European heat waves (1979–2019), Atmospheric Science Letters, 23, e1120, https://doi.org/10.1002/asl.1120, 2022.

Benson, D. O. and Dirmeyer, P. A.: Characterizing the Relationship between Temperature and Soil Moisture Extremes and Their Role in the Exacerbation of Heat Waves over the Contiguous United States, Journal of Climate, 34, 2175–2187, https://doi.org/10.1175/jcli-d-20-0440.1, 2021.

Bieli, M., Pfahl, S., and Wernli, H.: A Lagrangian investigation of hot and cold temperature extremes in Europe, Quarterly Journal of the Royal Meteorological Society, 141, 98–108, https://doi.org/10.1002/qj.2339, 2015.

Calvin, K., Dasgupta, D., Krinner, G., Mukherji, A., Thorne, P. W., Trisos, C., Romero, J., Aldunce, P., Barrett, K., Blanco, G., Cheung, W. W., Connors, S., Denton, F., Diongue-Niang, A., Dodman, D., Garschagen, M., Geden, O., Hayward, B., Jones, C., Jotzo, F., Krug, T., Lasco, R., Lee, Y.-Y., Masson-Delmotte, V., Meinshausen, M., Mintenbeck, K., Mokssit, A., Otto, F. E., Pathak, M., Pirani, A., Poloczanska, E., Pörtner, H.-O., Revi, A., Roberts, D. C., Roy, J., Ruane, A. C., Skea, J., Shukla, P. R., Slade, R., Slangen, A., Sokona, Y., Sörensson, A. A., Tignor, M., van Vuuren, D., Wei, Y.-M., Winkler, H., Zhai, P., Zommers, Z., Hourcade, J.-C., Johnson, F. X., Pachauri, S., Simpson, N. P., Singh, C., Thomas, A., Totin, E., Alegría, A., Armour, K., Bednar-Friedl, B., Blok, K., Cissé, G., Dentener, F., Eriksen, S., Fischer, E., Garner, G., Guivarch, C., Haasnoot, M., Hansen, G., Hauser, M., Hawkins, E., Hermans, T., Kopp, R., Leprince-Ringuet, N., Lewis, J., Ley, D., Ludden, C., Niamir, L., Nicholls, Z., Some, S., Szopa, S., Trewin, B., van der Wijst, K.-I., Winter, G., Witting, M., Birt, A., and Ha, M.: IPCC, 2023: Climate Change 2023: Synthesis Report. Contribution of Working Groups I, II and III to the Sixth Assessment Report of the Intergovernmental Panel on Climate Change [Core Writing Team, H. Lee and J. Romero (eds.)]. IPCC, Geneva, Switzerland., https://doi.org/10.59327/ipcc/ar6-9789291691647, 2023.

Dillerup, I., Lemburg, A., Buschow, S., and Pinto, J. G.: Dynamical system metrics and weather regimes explain the seasonally-varying link between European heatwaves and the large-scale atmospheric circulation, Earth System Dynamics, 17, 265–289, https://doi.org/10.5194/esd-17-265-2026, 2026.

Giuliani, N., Wegher, M., Asensio, D., Zanotelli, D., Andreotti, C., and Tagliavini, M.: Impact of soil water availability on apple tree physiology during heatwaves and on post-stress recovery, Environmental and Experimental Botany, 235, 106 161, https://doi.org/10.1016/j.envexpbot.2025.106161, 2025.

Grams, C. M.: A life cycle definition of year-round weather regimes in the North Atlantic European region, EGUsphere [preprint], 2026, 1–60, https://doi.org/10.5194/egusphere-2025-6385, 2026.

Hannachi, A., Straus, D. M., Franzke, C. L. E., Corti, S., and Woollings, T.: Low-frequency nonlinearity and regime behavior in the Northern Hemisphere extratropical atmosphere, Reviews of Geophysics, 55, 199–234, https://doi.org/10.1002/2015RG000509, 2017.

Hersbach, H., Bell, B., Berrisford, P., Biavati, G., Horányi, A., Muñoz Sabater, J., Nicolas, J., Peubey, C., Radu, R., Rozum, I., Schepers, D., Simmons, A., Soci, C., Dee, D., and Thépaut, J.-N.: ERA5 hourly data on single levels from 1940 to present, copernicus Climate Change Service (C3S) Climate Data Store (CDS), https://doi.org/10.24381/cds.adbb2d47, 2023.

https://doi.org/10.5194/egusphere-2026-2453
Preprint. Discussion started: 12 June 2026
© Author(s) 2026. CC BY 4.0 License.

Hughes, T. P., Kerry, J. T., Connolly, S. R., Baird, A. H., Eakin, C. M., Heron, S. F., Hoey, A. S., Hoogenboom, M. O., Jacobson, M., Liu, G., Pratchett, M. S., Skirving, W., and Torda, G.: Ecological memory modifies the cumulative impact of recurrent climate extremes, Nature Climate Change, 9, 40–43, https://doi.org/10.1038/s41558-018-0351-2, 2018.

Hundhausen, M., Feldmann, H., Laube, N., and Pinto, J. G.: Future heat extremes and impacts in a convection-permitting climate ensemble over Germany, Natural Hazards and Earth System Sciences, 23, 2873–2893, https://doi.org/10.5194/nhess-23-2873-2023, 2023.

Kautz, L.-A., Martius, O., Pfahl, S., Pinto, J. G., Ramos, A. M., Sousa, P. M., and Woollings, T.: Atmospheric blocking and weather extremes over the Euro-Atlantic sector – a review, Weather and Climate Dynamics, 3, 305–336, https://doi.org/10.5194/wcd-3-305-2022, 2022.

Lemburg, A., Fink, A. H., Lima, M. M., and Pinto, J. G.: Lagrangian analysis of two flavours of Central European heatwaves: Formation under omega blocking versus initiation by subtropical ridges, Quarterly Journal of the Royal Meteorological Society, n/a, e70 199, https://doi.org/10.1002/qj.70199, 2026.

León-FonFay, D., Lemburg, A., Fink, A. H., Pinto, J. G., and Feser, F.: A combined storyline-statistical approach for conditional extreme event attribution, Weather and Climate Dynamics, 7, 597–613, https://doi.org/10.5194/wcd-7-597-2026, 2026.

Liu, X., He, B., Guo, L., Huang, L., and Chen, D.: Similarities and Differences in the Mechanisms Causing the European Summer Heatwaves in 2003, 2010, and 2018, Earth's Future, 8, e2019EF001 386, https://doi.org/10.1029/2019EF001386, 2020.

Maraun, D., Schiemann, R., Ossó, A., and Jury, M.: Changes in event soil moisture-temperature coupling can intensify very extreme heat beyond expectations, Nature Communications, 16, 734, https://doi.org/10.1038/s41467-025-56109-0, 2025.

Messori, G., Segalini, A., and Ramos, A. M.: Climatology and trends of concurrent temperature extremes in the global extratropics, Earth System Dynamics, 15, 1207–1225, https://doi.org/10.5194/esd-15-1207-2024, 2024.

Michel, C. and Rivière, G.: The Link between Rossby Wave Breakings and Weather Regime Transitions, Journal of the Atmospheric Sciences, 68, 1730–1748, https://doi.org/10.1175/2011jas3635.1, 2011.

Perkins, S. E.: A review on the scientific understanding of heatwaves—Their measurement, driving mechanisms, and changes at the global scale, Atmospheric Research, 164-165, 242–267, https://doi.org/10.1016/j.atmosres.2015.05.014, 2015.

Perkins, S. E. and Alexander, L. V.: On the Measurement of Heat Waves, Journal of Climate, 26, 4500 – 4517, https://doi.org/10.1175/JCLI-D-12-00383.1, 2013.

Polazzo, F., Hermann, M., Crettaz-Minaglia, M., and Rico, A.: Recurrent Heatwaves Slow Down the Recovery of a Phytoplankton Community, Ecology and Evolution, 14, e70 539, https://doi.org/10.1002/ece3.70539, 2024.

Robinson, P. J.: On the Definition of a Heat Wave, Journal of Applied Meteorology, 40, 762 – 775, https://doi.org/10.1175/1520-0450(2001)040<0762:OTDOAH>2.0.CO;2, 2001.

Russo, S., Sillmann, J., and Fischer, E. M.: Top ten European heatwaves since 1950 and their occurrence in the coming decades, Environmental Research Letters, 10, 124 003, https://doi.org/10.1088/1748-9326/10/12/124003, 2015.

Sales, K., Vasudeva, R., and Gage, M. J. G.: Fertility and mortality impacts of thermal stress from experimental heatwaves on different life stages and their recovery in a model insect, Royal Society Open Science, 8, https://doi.org/10.1098/rsos.201717, 2021.

Santos, J. A., Pfahl, S., Pinto, J. G., and Wernli, H.: Mechanisms underlying temperature extremes in Iberia: a Lagrangian perspective, Tellus A: Dynamic Meteorology and Oceanography, 67, 26 032, https://doi.org/10.3402/tellusa.v67.26032, 2015.

Seneviratne, S. I., Corti, T., Davin, E. L., Hirschi, M., Jaeger, E. B., Lehner, I., Orlowsky, B., and Teuling, A. J.: Investigating soil moisture–climate interactions in a changing climate: A review, Earth-Science Reviews, 99, 125–161, https://doi.org/10.1016/j.earscirev.2010.02.004, 2010.

https://doi.org/10.5194/egusphere-2026-2453
Preprint. Discussion started: 12 June 2026
© Author(s) 2026. CC BY 4.0 License.

Sharpe, L., Cale, B., and Gardner, J. L.: Weighing the cost: the impact of serial heatwaves on body mass in a small Australian passerine, Journal of Avian Biology, 50, https://doi.org/10.1111/jav.02355, 2019.

Sánchez-Benítez, A., Barriopedro, D., and García-Herrera, R.: Tracking Iberian heatwaves from a new perspective, Weather and Climate Extremes, 28, 100 238, https://doi.org/10.1016/j.wace.2019.100238, 2020.

Zhang, L., Liao, W., Chen, X., Cheng, S., and Yang, J.: Temporally Compound Heatwave and Its Interaction With Urban Heat Island Over Mainland China, Earth's Future, 13, e2025EF006 490, https://doi.org/10.1029/2025EF006490, 2025.

Zscheischler, J., Martius, O., Westra, S., Bevacqua, E., Raymond, C., Horton, R. M., van den Hurk, B., AghaKouchak, A., Jézéquel, A., Mahecha, M. D., Maraun, D., Ramos, A. M., Ridder, N. N., Thiery, W., and Vignotto, E.: A typology of compound weather and climate events, Nat. Rev. Earth Environ., 1, 333–347, https://doi.org/10.1038/s43017-020-0060-z, 2020.